J. Electrochem. Sci. Eng. **15(2)** (2025) 2262; http://dx.doi.org/10.5599/jese.2262

Open Access : : ISSN 1847-9286
https://pub.iapchem.org/ojs/index.php/JESE

Original scientific paper

Comparative voltammetric determination of ascorbic acid at three different carbon electrodes: application of carbon screen-printed electrode for citrus fruits analysis

Talytha Rodrigues Gaspari Paina[1], Izabel Cristina Eleotério[1], Nelson Ramos Stradiotto[2] and Marcelo Firmino de Oliveira[1,✉]

[1]*Grupo de Eletroquímica, Eletroanalítica e Química Forense (GEEQFor), Departamento de Química, Faculdade de Filosofia, Ciências e Letras de Ribeirão Preto, Universidade de São Paulo (DQ/FFCLRP/USP), Avenida Bandeirantes, 3900, Bairro Monte Alegre, Ribeirão Preto, SP, CEP 14040-901, Brazi*

[2]*Instituto de Química - Universidade Estadual Paulista (IQ-UNESP). Av. Prof. Francisco Degni, 55 - Jardim Quitandinha, Araraquara, SP, CEP 14800-900, Brazil*

Corresponding author: ✉marcelex@usp.br

Received: January 29, 2024; Accepted: February 22, 2025; Published: March 3, 2025

Abstract

Determining the vitamin C (ascorbic acid) content in citrus fruits is crucial for dietary and nutritional considerations. Traditional analytical methods for ascorbic acid analysis often involve expensive and less portable electrodes, limiting their practicality in food analysis. This study focuses on the quantification of ascorbic acid in citrus fruits using a cost-effective and portable carbon screen-printed electrode. The efficiency of these electrodes was assessed using cyclic voltammetry and linear sweep voltammetry due to the irreversible oxidation behavior of ascorbic acid. A comparative analysis was performed with glassy carbon, carbon paste, and commercial carbon screen-printed electrodes, focusing on sensitivity variations based on analyte concentration and scanning rate. The carbon screen-printed electrode demonstrated superior sensitivity to the other electrodes tested, establishing it as a practical alternative for ascorbic acid analysis in citrus fruits. This study employed the standard addition method in conjunction with linear sweep voltammetry to accurately determine ascorbic acid concentrations in pear-orange, Tahiti lemon, and Ponkan tangerine samples. The obtained values were cross-referenced with existing literature data, enhancing our understanding of vitamin C content in these citrus fruits. Overall, this research highlights the potential of the carbon screen-printed electrode as a valuable tool for vitamin C analysis, offering new insights into food science and nutrition.

Keywords

Vitamin C; carbon electrodes; voltammetry techniques; standard addition method; juice samples

Introduction

Vitamin C, also known as ascorbic acid (AA), is a water-soluble essential nutrient with profound physiological significance. It assumes the form of the biologically active L-enantiomer, L-ascorbic acid, featuring a γ-lactone structure. Under physiological conditions, ascorbic acid exhibits a hexanoic sugar acid structure and maintains its ionic state as the ascorbate anion due to the presence of two dissociable protons, characterized by pKa values of 4.17 and 11.57 [1].

L-ascorbic acid readily oxidizes, forming the basis for its electrochemical detection. It establishes an irreversible redox pair with dehydroascorbic acid [1]. The acidity of AA is influenced by the conjugation of the carbonyl on carbon 1, notably enhancing the acidity of the hydroxyl on carbon 3 (pK_a = 4.17), while the hydroxyl on carbon 2, as part of an enol, exhibits equivalent acidity with a pKa of 11.57 [2-4]

Vitamin C has diverse properties, including its redox capabilities**,** which play a crucial role in electrochemical, biochemical, and pharmacological systems. It serves as a potent antioxidant, combating diseases caused by free radicals, such as heart disease [1]. Additionally, it contributes to iron absorption, collagen synthesis for cell growth and regeneration, immune response activation, wound healing, osteogenesis, and the maintenance of capillaries, bones, and teeth. Notably, humans, along with certain primates and guinea pigs, rely on dietary intake due to a genetic mutation that prevents the synthesis of ascorbate (the anionic portion of AA).

Given the paramount importance of vitamin C, various methods are employed to detect and quantify it, including spectroscopy, chromatography, and electrochemistry. In electrochemistry, carbon materials are highly exploited as electrode surfaces. This is due to the fact that, in addition to being chemically inert and low-cost compared to other materials, carbon materials also have a low background current and a wide potential window.

The glassy carbon electrode (GCE), sometimes referred to as a "conventional" electrode, has large overpotentials for oxygen and hydrogen evolution and is chemically stable. Compared to the carbon paste electrode (CPE), for example, it has, according to studies, much higher currents, even though both electrodes have the same surface área [1]. However, the CPE has a significantly lower background current, which makes it superior to glassy carbon from the point of view of background signal characteristics. In addition, it offers few beneficial properties, including repeatability, stability, and surface renewability, and has been explored by several authors [5,6], who have proven its effectiveness in both bare and modified forms.

However, while traditional electrochemical techniques with GCE and CPE offer high sensitivity, commercial carbon screen-printed electrodes (C-SPEs) have emerged as a more practical, easy-to-use, cost-effective, and efficient alternative. Recent studies, including [7], have demonstrated superior current responses C-SPEs compared to unmodified GCE, as well as its practicality, saving the effort, time and materials spent preparing a good carbon paste to be used as a CPE. Furthermore, the versatility of screen-printed electrodes has led to their increased application in analyzing a wide range of samples, simplifying the detection process by requiring only a solubilized matrix drop, such as powder or tablet [7].

Therefore, this study aims to compare the oxidation behavior of ascorbic acid using three carbon electrodes shown in Figure 1, *i.e.* GCE, CPE and C-SPE, highlighting their respective advantages and disadvantages. Citrus fruits, including pear-orange, Tahiti lemon, and Ponkan tangerine, served as the sample matrix, and the analysis employed cyclic voltammetry (CV) and linear sweep voltammetry (LSV) techniques, using C-SPE as the working electrode after proving its efficiency compared to other carbon electrodes.

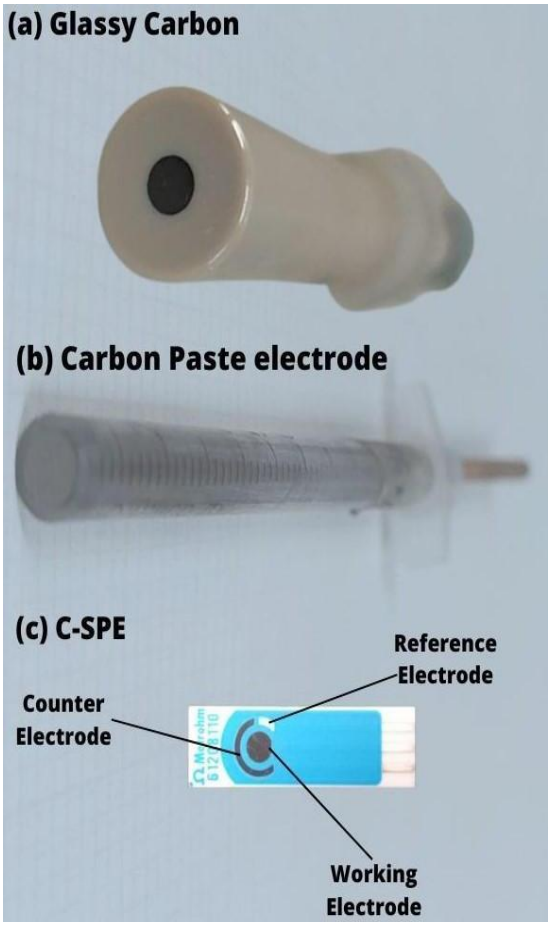

Figure 1. *Electrodes used for the electrochemical setup: (a) glassy carbon electrode; (b) carbon paste electrode; (c) carbon screen-printed electrode wire as working electrode, reference electrode and auxiliary electrode*

Experimental

Electrochemical setup

The experiments employed a glass cell equipped with three electrodes, a Metrohm® saturated Ag/AgCl/KCl, 3 mol L^{-1} reference electrode, a platinum wire auxiliary electrode, and GCE, CPE, and C-SPE as working electrodes, each with a physical area of 0.0707 cm^2. The electrolyte solution, prepared in-house using Sigma Aldrich products, consisted of a 0.1 mol L^{--1} buffer solution of potassium phosphate monobasic (99 % purity) and sodium phosphate dibasic heptahydrate (99 % purity), adjusted to pH 5.5 using a Mettler Toledo digital bench pH-meter, which has been used in other studies that have proven its effectiveness, due to the presence of ionizable hydrogens in the structure of the ascorbic acid molecule [2]. The active surface area of GCE, CPE, and C-SPE was calculated using the Randles-Ševčik equation [8] with 5 mmol L^{-1} $K_3[Fe(CN)_6]$ in 0.5 mol L^{-1} KCl, at scan rates ranging from 5 to 200 mV s^{-1}, resulting in areas of 0.027, 0.044 and 0.063 cm^2, respectively.

Carbon paste electrode preparation

The CPE was created by blending 0.35 g of graphite powder (Fisher Scientific, 99.9 % purity) with 0.15 g of paraffin (Sigma Aldrich) at a 7:3 weight ratio. The mixture was heated in a mortar over a heating mantle at approximately 100 °C until it formed a paste, which took about 10 minutes. This paste was then packed into a cylindrical plastic tube resembling a syringe and compressed using a copper rod. Finally, the electrode surface was polished using abrasive paper, resulting in a 3 mm diameter electrode.

Standard ascorbic acid preparation

The chemical structure of AA is drawn in Figure 2a. For the analysis of AA oxidation profiles using carbon working electrodes, a 0.1 mol L^{-1} AA standard solution was prepared by dissolving 0.4403 g of standard AA (100 % purity) from Sigma-Aldrich in 25 mL of deionized water using a 25 mL flask.

Analysis of standard ascorbic acid with glassy carbon electrode

For standard AA analyses, 100 µL aliquots of the 0.1 mol L^{-1} AA solution were sequentially added to 10 mL of 0.1 mol L^{-1} phosphate buffer (pH 5.5), serving as the electrolyte in an electrochemical cell. The glassy carbon electrode, 3 mm diameter, from Metrohm®, was employed as the working electrode. Cyclic voltammograms were recorded after each 100 µL AA addition to confirm the irreversibility of the oxidation process. This was done by varying AA concentration at the constant scan rate, and subsequently, the scan rate varied at a constant AA concentration. Experimental conditions for cyclic voltammetry included scanning rates of 50 mV s^{-1} for concentration analysis (ranging from 0.99 to 4.76 mmol L^{-1}) and 5, 10, 25, 50 and 100 mV s^{-1} for scan rate analysis, maintaining a fixed final AA concentration of 4.76 mmol L^{-1}. The potential range was set from -0.4 to +0.9 V, with a current scale of 5 mA.

Analysis of standard ascorbic acid with carbon paste electrode

At this stage, five 100 µL aliquots of the 0.1 mol L^{-1} AA standard solution were added to 10 mL of 0.1 mol L^{-1} phosphate buffer, pH 5.5, which acted as the electrolyte in the electrochemical cell, using the CPE as the working electrode. Linear voltammograms were then generated for the addition of 100, 200, 300, 400 and 500 µL of AA solution. The experimental conditions for the linear sweep voltammetry were a scanning rate of 50 mV s^{-1} in the concentration variation analysis, which ranged from 0.99 to 4.76 mmol L^{-1}. As for GCE, potential scan rates of 5, 10, 25, 50 and 100 mV s^{-1} were applied in the rate variation analysis with a fixed final concentration of 4.76 mmol L^{-1} of the AA standard. The potential range was between -0.2 and +1.5 V, with a current scale of 5 mA.

Analysis of standard ascorbic acid with carbon screen-printed electrode

A 3 mm diameter carbon screen-printed electrode with Metrohm®'s patented carbon ink was used as a working electrode. To enhance peak quality, larger volumes (ranging from 11 to 15 µL) of the 0.1 mol L^{-1}AA standard solution were added to a fixed volume of 0.1 mol L^{-1} phosphate buffer, pH 5.5, to increase the sample concentration in the analysis. Experimental conditions for LSV included potential scanning rates of 50 mV s^{-1} for concentration analysis (ranging from 23.9 to 30 mmol L^{-1}) and 5, 10, 25, 50 and 100 mV s^{-1} for the scan rate analysis, maintaining a constant final AA concentration of 30 mmol L^{-1}. The potential range was set between -0.4 and +1.1 V, with a current scale of 5 mA.

Comparison of standard ascorbic acid analysis using three electrodes

First, to carry out the standard ascorbic acid analyses, five 0.5 µL aliquots of the 0.1 mol L^{-1} ascorbic acid standard solution were added to a fixed volume of 0.1 mol L^{-1} phosphate buffer, pH 5.5, which acted as the electrolyte in the electrochemical cell, using C-SPE as the working electrode again. Linear voltammograms were generated with the same concentrations previously calculated for GCE and CPE. Experimental conditions for linear sweep voltammetry included potential scanning rates of 50 mV s^{-1} for concentration analysis (ranging from 0.99 to 4.76 mmol L^{-1}). The potential range was set between -0.4 and +1.1 V, with a current scale of 5 mA.

Next, to compare the signals obtained from the three electrodes, all with 3 mm diameter, the same AA concentration was utilized for each. Experimental conditions for LSV included fixed AA

concentration (4.76 mmol L^{-1}) for all three electrodes, scan rates of 50 mV s^{-1}, potential range from 0.0 to +1.0 V, and a current scale of 5 mA.

Cyclic voltammetry and linear sweep voltammetry

Cyclic voltammetry and linear sweep voltammetry techniques were chosen to study the oxidation of ascorbic acid in standard solutions and citrus fruits due to the simplicity of these two techniques, which were sufficient for the qualitative and quantitative analysis of the analyte. Metrohm® AUTOLAB 128N potentiostat coupled to a computer was used for data acquisition.

Preparation and analysis of ascorbic acid in citrus fruits

Fruit juice was extracted using a manual juicer, filtered, and then combined with phosphate buffer solution pH 5.5 (0.1 mol L^{-1}). An 18 µL aliquot of the mixture was added to the working electrode region of the C-SPE for AA determination using the standard addition method. Different standard AA solutions (0.05 mol L^{-1} for pear-orange, 0.1 mol L^{-1} for Tahiti lemon, and 0.05 mol L^{-1} for Ponkan tangerine) were employed. LSV was conducted with a potential range from -0.4 to +1.2 V, a scan rate of 50 mV s^{-1}, and a current scale of 5 mA.

Results and discussion

Analysis of standard ascorbic acid using GCE

The AA oxidation profile at GCE was analyzed as the concentration varied. Figure 2b shows that in higher sample concentrations, the anodic current at +0.6 V rises proportionally to electrolyte concentration, which is in line with theoretical expectations [9]. The potential shift observed corresponds to concentration changes, affirming the irreversible nature of the AA oxidation process. This data was used to construct a concentration-current graph.

In this study, the graph depicts a linear relationship between current and AA concentration, which aligns with the expected irreversibility of the reaction [10]. The linear fit equation, $y = a + bx$, provides the angular (b = 8.72 µA mmol L^{-1}) and linear (a = 6.27 µA) coefficients. AA signal increased with concentration, resulting in one well-defined linear range, as displayed in Figure 2c.

The high Pearson correlation coefficient (r = 0.953) signifies a strong positive correlation between analyte concentration and current intensity, indicating their direct proportionality. Finally, the limit of detection (LoD), representing the minimum detectable concentration, can be calculated using the equation proposed by [9]. The limit of detection is calculated using the equation LoD = $3s/m$, where 3 is the confidence factor, s represents the standard deviation of the blank, and m stands for the angular coefficient of the analytical curve. By substituting the given values into the equation, the LoD is determined by Equation (1):

$$\text{LoD} = 3s/m = (3\times5.1\ \mu\text{A})/(35\ \mu\text{A}/(4.76\text{-}0.99)\ \text{mmol}\ L^{-1}) = 1.64\ \text{mmol}\ L^{-1} \quad (1)$$

The determined limit of detection (LoD) at GCE of 1.64 mmol L^{-1} is higher than the initial addition of AA at 0.99 mmol L^{-1}, which indicates that the chosen analyte quantities did not significantly differ from the blank (phosphate buffer solution at pH 5.5). The LoD represents the lowest concentration distinguishable from the electrolyte with a high level of confidence. Consequently, concentrations below the detection limit should be considered less reliable. Specifically at GCE, only the concentration of 0.99 mmol L^{-1} cannot be readily distinguished from the blank, while concentrations ranging from 1.96 to 4.76 mmol L^{-1} surpass LoD and are considered valid.

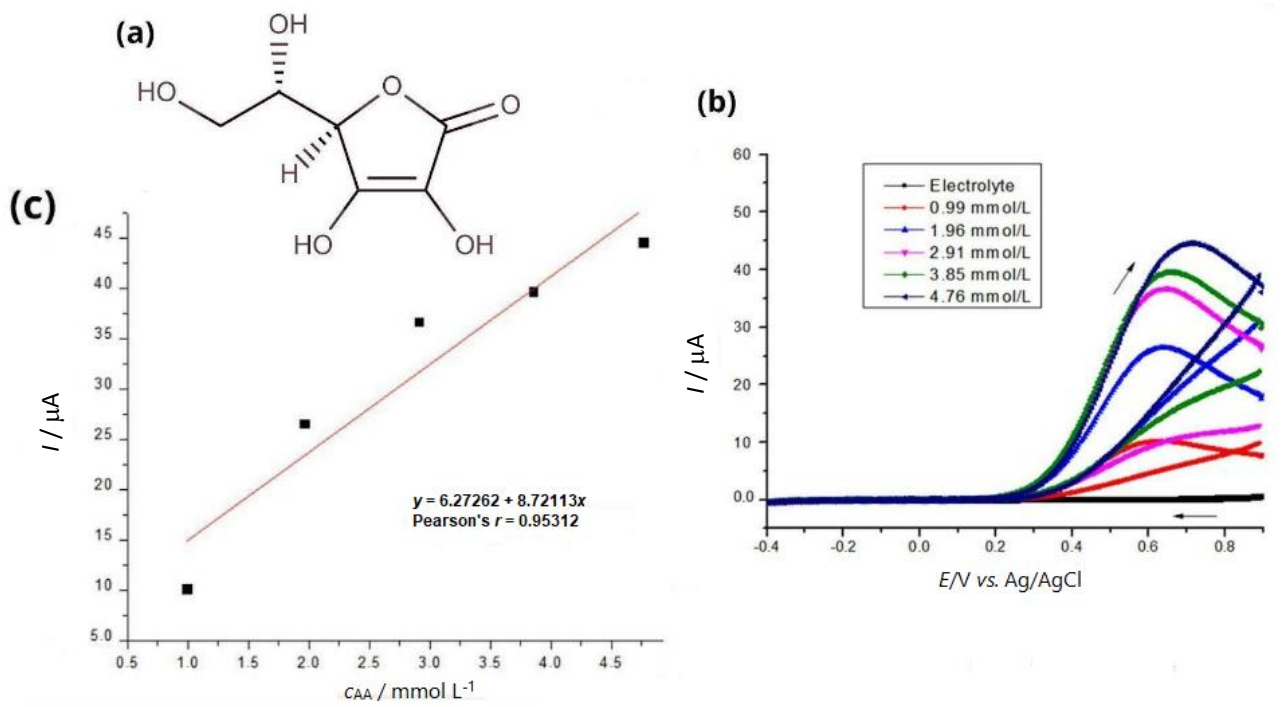

Figure 2. *(a) Chemical structure of AA; (b) cyclic voltammograms at 50 mV s^{-1} of GCE in 0.1 mol L^{-1} phosphate buffer, pH 5.5, and varying the final AA concentration from 0.99 to 4.76 mmol L^{-1}; (c) linear correlation between peak current and AA concentration*

Following this, the oxidation behavior of AA was examined with varying potential scan rates (Figure 3a). The oxidation potential in these voltammograms shifts towards more positive values, surpassing +0.6 V (potential associated with the occurrence of anodic current peaks)—as both the scan rate and concentration rise. Additionally, it is evident that the intensity of the anodic peak current escalates with a higher scan rate. Using this data, a relationship between the peak current (i_p) and the square root of the scan rate ($v^{1/2}$) is illustrated in Figure 3b. A closer examination of the variation of peak current with the scan rate shows a linear correlation between the peak current and the square root of the scan rate (r = 0.99). This indicates that the oxidation process occurring on the electrode surface is primarily diffusion-controlled rather than adsorption-controlled—the latter being the alternative possibility. This finding aligns with previous studies [2] that have similarly drawn this conclusion.

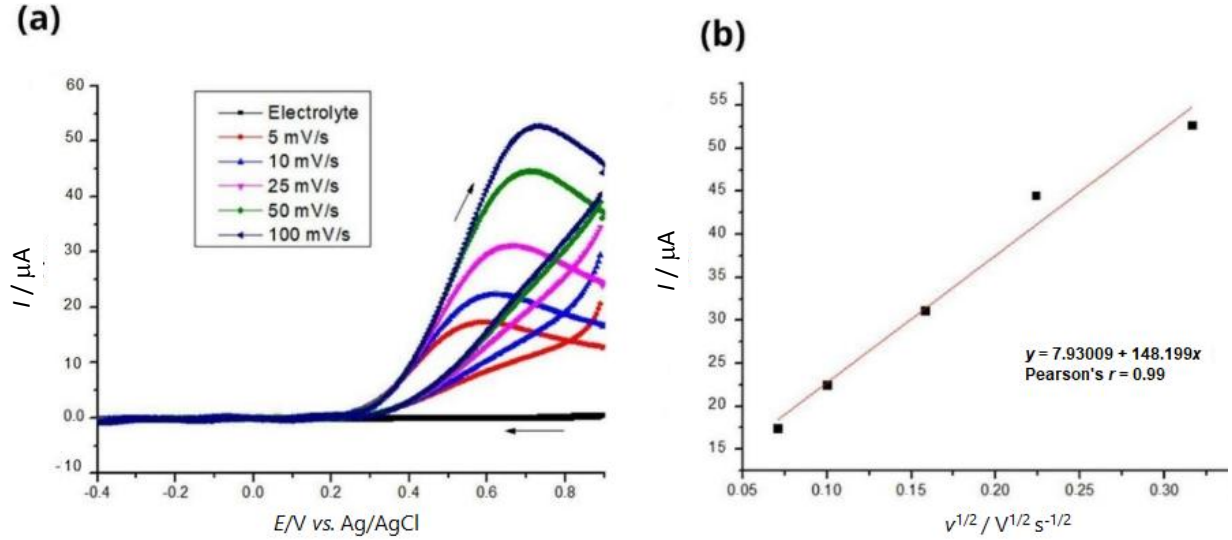

Figure 3. *(a) Effect of scan rate on cyclic voltammetric response of GCE in 0.1 mol L^{-1} phosphate buffer, pH 5.5, and final AA concentration of 4.76 mmol L^{-1}; (b) linear plot of peak current vs. square root of scan rate*

Analysis of standard ascorbic acid using CPE

The AA oxidation profile was scrutinized for concentration variations, this time employing the CPE. Similar to the GCE, anodic peaks emerged upon adding aliquots of the AA solution, signifying its oxidation. These peaks are manifested at +0.75 V, denoting the potential at which AA undergoes oxidation, as confirmed by the recorded electron transfer. Notably, there was a slight shift in oxidation potential, transitioning from 0.6 to 0.75 V in comparison to the peaks observed with the GCE. This shift was attributed to the excess of paraffin in the CPE, which acts as a binder, filling the interstitial spaces between the particles and consequently adjusting the AA oxidation reaction to a slightly higher potential. Subsequently, mirroring the procedure with the GCE, a graph correlating current with concentration was constructed using the standard AA (Figure 4a). This graph reaffirms the linear relationship between the current (µA) and the concentration of AA (mmol L^{-1}) (Figure 4b), as expected for an irreversible reaction [10]. Utilizing the linear fit equation, $y = a + bx$, we derived the values of b and a, corresponding to the angular and linear coefficients of the line, respectively. These values were b = 14.17 µA mmol L^{-1} and a = 14.58 µA.

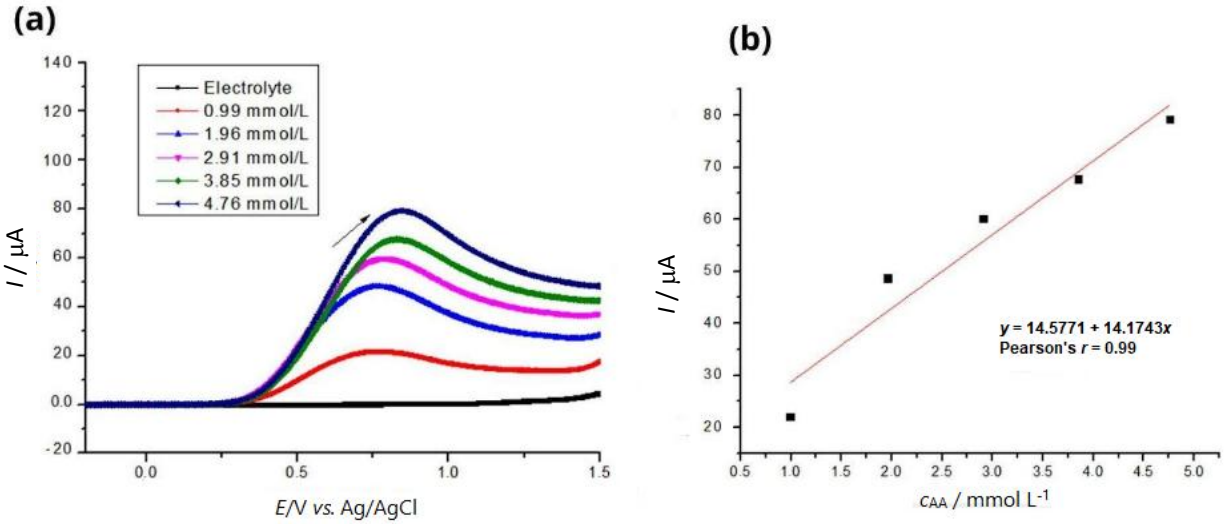

Figure 4. *(a) Linear sweep voltammograms (LSV) at 50 mV $s^{-1}$of CPE in 0.1 mol L^{-1} phosphate buffer, pH 5.5, and varying the AA final concentration from 0.99 to 4.76 mmol L^{-1}; (b) linear correlation between peak current and AA concentration*

As previously mentioned, the closer the correlation coefficient is to 1, the stronger the linearity between the two variables. Consequently, the coefficient determined using the analytical curve, $r = 0.97$, confirms this linearity and establishes the direct proportionality between electrolyte concentration and current intensity. Finally, the limit of detection (LoD) was calculated by Equation (2):

$$\text{LoD} = 3s/m = (3 \cdot 6.5\ \mu\text{A})/((60\ \mu\text{A}/(4.76\text{-}0.99)\ \text{mmol L}^{-1}) = 1.2\ \text{mmol L}^{-1} \quad (2)$$

The determined LoD is 1.2 mmol L^{-1} , which is a value above the AA concentration of the first addition (0.99 mmol L^{-1}) and below the others, demonstrating that the amounts of analytes chosen were significantly different from the blank (electrolyte-phosphate buffer solution pH 5.5), with the exception of the first addition, which is unreliable. Therefore, the results for CPE could be validated only for concentrations between 1.96 and 4.76 mmol L^{-1}.

In the following, the analysis of AA oxidation was extended to varying scan rates, now for the CPE (Figure 5a). This dataset facilitated the creation of linear plots illustrating peak potential against the square root of the scan rate (Figure 5b). From this graph, a direct correlation was evident between the peak current and the square root of the scanning rate (r = 0.987). This indicates that the

oxidation process on the electrode surface primarily follows a diffusion-controlled reaction rather than an adsorption-controlled one. This observation aligns with previous findings using the glassy carbon electrode and is consistent with conclusions drawn in other studies [2].

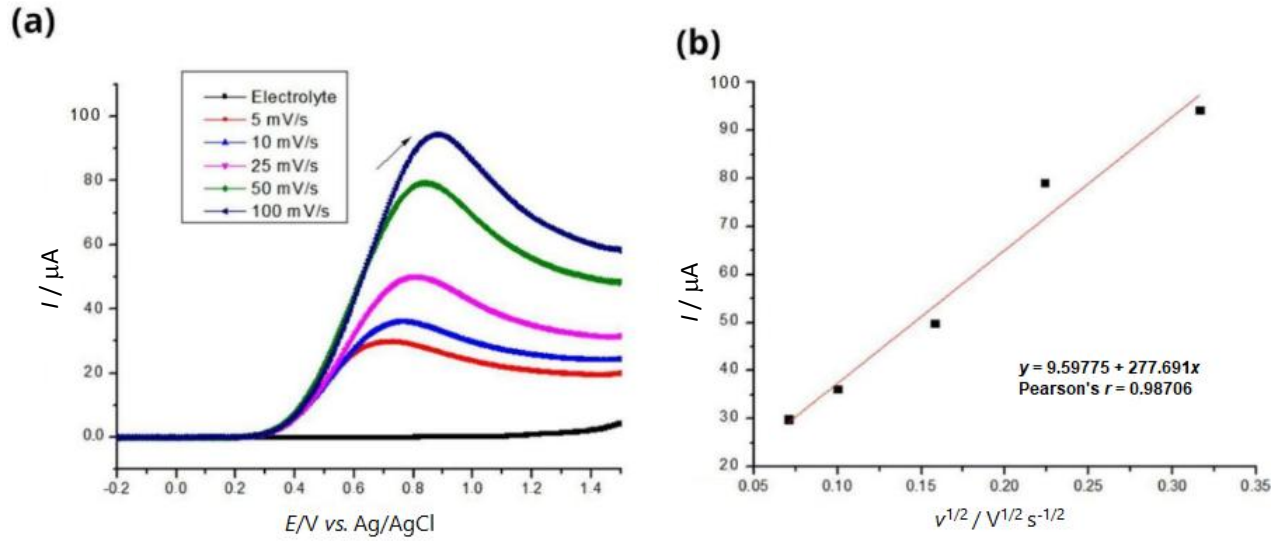

Figure 5. *(a) Effect of scan rate (5 to 100 mV s^{-1}) on LSV responses of CPE in 0.1 mol L^{-1} phosphate buffer, pH 5.5, and final AA concentration of 4.76 mmol L^{-1}; (b) linear plot of peak current* vs. *square root of scan rate*

Analysis of standard ascorbic acid using carbon screen-printed electrode

To compare the three electrodes, an analysis was carried out using standard ascorbic acid at somewhat higher concentrations than those used for GCE and CPE in order to ensure its electrochemical response.

In this phase, the oxidation profile of AA was scrutinized with varying concentrations. With new volumes of standard AA solution, the anodic peaks shifted to a potential of +0.8 V. This shift was attributed to the escalated AA concentrations. Additionally, it was noted that the anodic current surged in tandem with concentration increments. This observation aligns with the previously emphasized principle that conductivity is directly linked to analyte concentration [9].

Upon the completion of the analyses utilizing the standard AA, a graph correlating current to concentration was developed, mirroring the procedure applied to the other electrodes (Figure 6b). Once again, the linearity between peak current (µA) and the concentration of AA (mmol L^{-1}) was evident [10]. Through the equation derived from the linear fit, $y = a + bx$, we derived the coefficients b and a. Specifically, the angular and linear coefficients were determined to be b = 16.4118 µA mmol L^{-1} and a = -77.7762 µA, respectively (Figure 6b).

The obtained Pearson correlation coefficient (r = 0.983) from the analytical curve affirms a direct proportionality between the electrolyte concentration and current intensity. Moving on to the calculation of the limit of detection (LoD), a critical parameter for sensitivity, since it is the smallest amount of analyte in the test sample that can be truly distinguished from zero, Equation (3) [9] is applied:

$$\text{LoD} = 3s/m = (3 \cdot 47.9\ \mu\text{A})/(115\ \mu\text{A}/(30\text{-}23.9)\ \text{mmol L}^{-1}) = 7.63\ \text{mmol L}^{-1} \quad (3)$$

LoD value of 7.63 mmol L^{-1} is notably lower than the initial AA concentration of 23.9 mmol L^{-1} introduced, underscoring the robust sensitivity of the printed electrode. This ensures that the selected analyte concentrations were significantly distinct from the blank (electrolyte-phosphate buffer solution at pH 5.5), substantiating the validity of the obtained results.

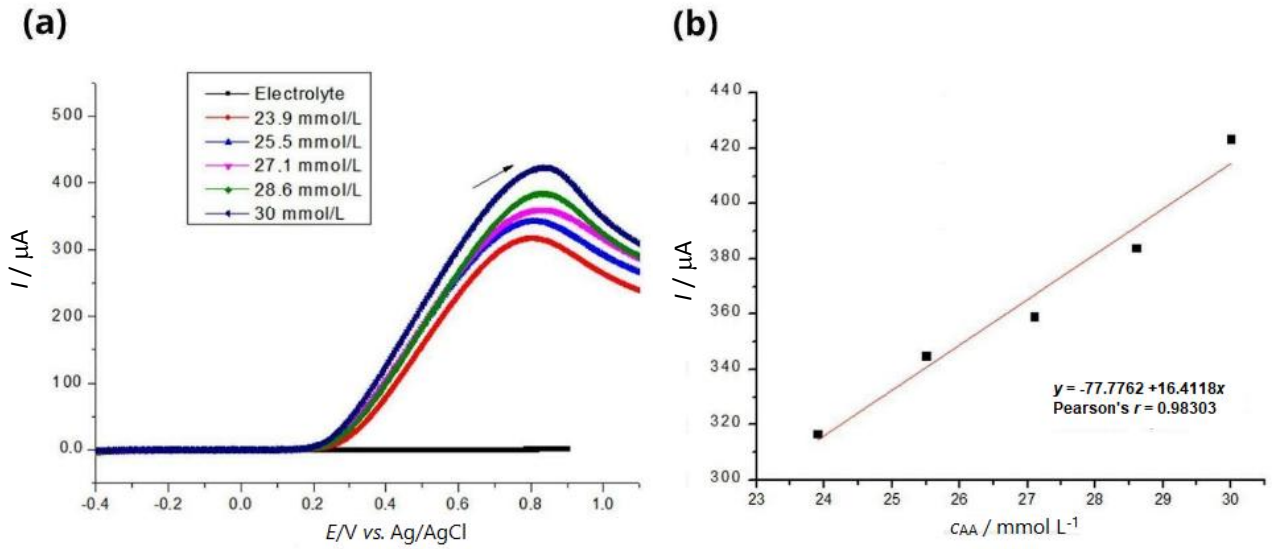

Figure 6. *(a) LSV curves at 50 mV s^{-1} of C-SPE in 0.1 mol L^{-1} phosphate buffer, pH 5.5, and varying the AA final concentration from 23.9 to 30 mmol L^{-1}; (b) linear correlation between peak current and AA concentration*

To investigate the behavior of ascorbic acid oxidation concerning varying scan rates, Figure 7a stands as a crucial source of insights. The voltammograms within the figure distinctly portray a notable trend, a discernible shift in the oxidation potential towards more positive values as the scan rate progressively increases. Alongside this observation, it becomes evident that the anodic peak current experiences a surge in intensity concomitant with the escalating scan rates. It is worth noting that a scan rate of 50 mV s^{-1} was employed in the other experiments, and as a result, the additional peaks linked with the carbon screen-printed electrode (C-SPE) were distinctly identified at a potential of 0.8 V.

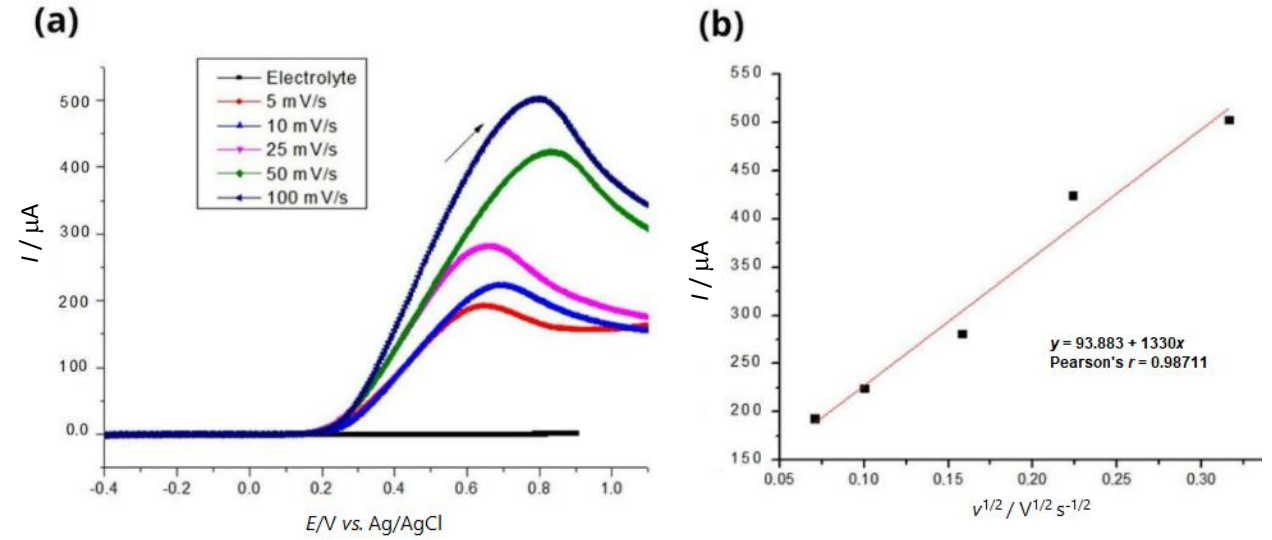

Figure 7. *(a) Effect of scan rate on LSV responses of C-SPE in 0.1 mol L^{-1} phosphate buffer, pH 5.5, and final AA concentration of 30 mmol L^{-1}; (b) linear plot of peak current vs. square root of scan rate*

Valuable insights into the oxidation behavior of ascorbic acid under varying scan rates can be obtained from LSV curves presented in Figure 7a. A graph depicting the peak current in relation to the square root of the potential sweep rate ($v^{½}$) is presented in Figure 7b, unveiling a strikingly linear relationship between the peak current and the square root of the scan rate (with a correlation coefficient of r = 0.987). This observation indicates that the oxidation process transpiring on the electrode surface is predominantly governed by diffusion as opposed to adsorption. This finding is

in alignment with prior observations utilizing GCE, CPE, and corroborating studies [2], which have likewise arrived at a similar conclusion. This insight further contributes to the comprehensive understanding of the intricacies governing the oxidation behavior of ascorbic acid.

Comparison of standard ascorbic acid analysis using the three electrodes

To compare the three electrodes, an analysis was carried out using standard ascorbic acid in the same concentrations as those used for GCE and CPE. It can be seen that using C-SPE at lower concentrations, the anodic peaks showed potentials of +0.3 V to +0.6 V. As shown in the previous analyses, this shift occurs as the concentration of ascorbic acid increases.

Again, a graph correlating current to concentration was developed, from which it is possible to observe the linearity between peak current (µA) and the concentration of AA (mmol L^{-1}). Using the equation derived from the linear fit, $y = a + bx$, it is possible to obtain the angular and linear coefficients, which correspond to b = 28.7375 µA mmol L^{-1} and a = -5.69623 µA, respectively (Figure 8b).

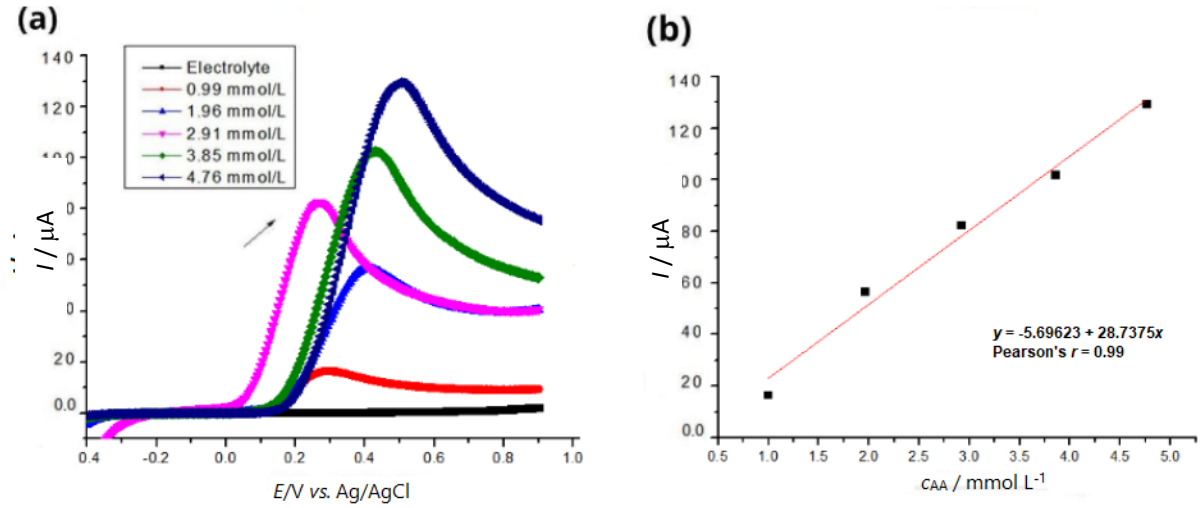

Figure 8. *(a) LSV curves at 50 mV s^{-1} of C-SPE in 0.1 mol L^{-1} phosphate buffer, pH 5.5, and varying the AA final concentration from 0.99 to 4.76 mmol L^{-1}; (b) linear correlation between peak current and AA concentration*

The obtained Pearson correlation coefficient (r = 0.99) from the analytical curve affirms a direct proportionality between the electrolyte concentration and current intensity. Moving on to the calculation of the limit of detection (LoD), a critical parameter for sensitivity, since it is the smallest amount of analyte in the test sample that can be truly distinguished from zero, the equation by [9] is applied:

$$\text{LoD} = 3s/m = (3 \cdot 6.32404\ \mu\text{A})/(120\ \mu\text{A}/(4.96\text{-}0.99)\ \text{mmol L}^{-1}) = 0.63\ \text{mmol L}^{-1} \quad (3)$$

The determined LoD is 0.63 mmol L^{-1}, a value lower than the initial AA concentration of 0.99 mmol L^{-1} introduced, underscoring again the robust sensitivity of the printed electrode, demonstrating that the selected analyte concentrations were significantly distinct from the blank (electrolyte-phosphate buffer solution at pH 5.5) and proving the validity of the obtained results.

Finally, comparing the three electrodes, GCE, CPE and C-SPE, at the same concentration of 4.76 mmol L^{-1}, we obtain the results shown by the voltammograms in Figure 9. A notable potential shift was observed in the three voltammograms. It transitioned from +0.5 to +0.7 V when moving from the C-SPE to the GCE and then further to +0.8 V from the GCE to the CPE. In an intriguing departure from theoretical expectations [1], the anodic peak current registered for the CPE (80 µA) exceeded that of the GCE (52.9 µA). This trend persisted across all other concentrations and rates.

This inversion suggests that the custom-made electrode demonstrated heightened sensitivity compared to the conventional electrode, possibly attributed to the lower ohmic resistance of the paste in contrast to the GCE.

In addition, the C-SPE demonstrated a notably higher current response, registering at 129 µA, compared to the unmodified GCE. This observation aligns with the anticipated outcomes as indicated in prior research [11]. Furthermore, it surpassed the peak current recorded by the CPE, showcasing superior sensitivity in comparison to the other electrodes.

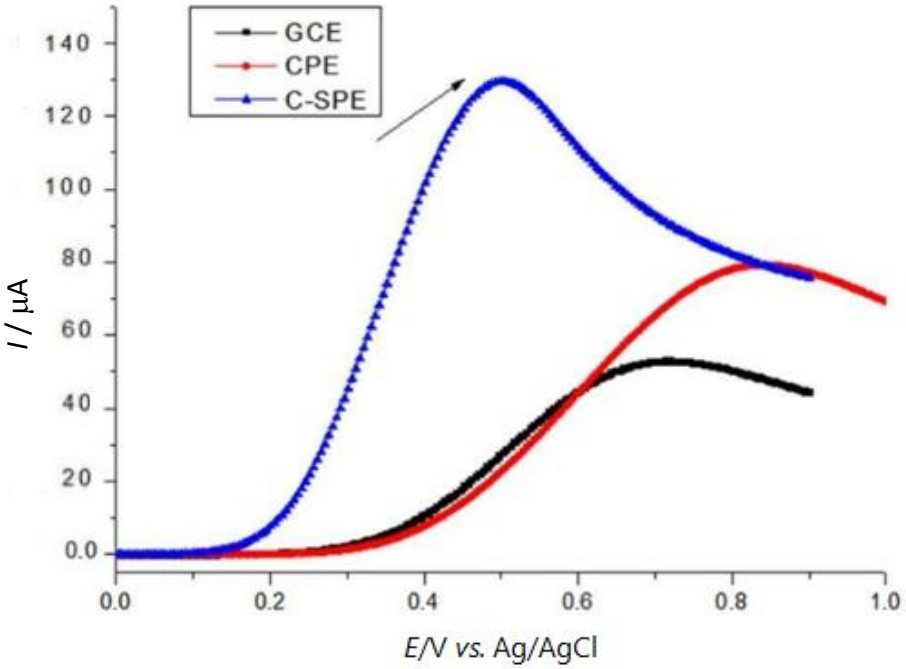

Figure 9. *LSV curves at 50 mV s^{-1} of GCE, CPE and C-SPE in 0.1 mol L^{-1} phosphate buffer, pH 5.5, with the AA final concentration 4.76 mmol L^{-1}*

It is worth noting that all electrodes proved efficient in generating the AA oxidation profile. They exhibited high sensitivity while maintaining a low background current, indicating minimal noise interference in the readings.

Determining the concentration of ascorbic acid in different juice samples using C-SPE

Due to its superior characteristics, as shown in the comparison above, C-SPE was used for AA determination in different juice samples (pear-orange, Tahiti lemon, and Ponkan tangerine). A standard addition method was employed, following a well-established protocol in which a sample of unknown initial concentration of analyte C_{X_i} exhibits a signal intensity of I_X. Subsequently, a precisely measured quantity of known standard S is introduced into an aliquot of the sample, resulting in an observed signal denoted as I_{S+X} for this solution. The addition of the standard induces a change in the original concentration of the analyte due to dilution.

Application of standard addition method for ascorbic acid quantification

For notation purposes, let C_{X_f} represent the diluted concentration of the analyte, where 'f' signifies "final". Similarly, the concentration of the standard in the final solution is denoted as C_{S_f}. It is important to note that the chemical species X and S are identical [9]. As per the fundamental principle, the signal is directly proportional to the concentration of the analyte.

The standard addition method involves adding known concentrations of a standard solution to a sample with an unknown initial concentration of the analyte, ascorbic acid. This process results in a change in the original concentration of the analyte due to dilution, allowing for precise determination. Equation (4) represents this relationship:

$$\frac{C_{X_i}}{C_{S_f}+C_{X_f}}=\frac{I_X}{I_{S+X}} \tag{4}$$

The equation above shows that the signal is directly proportional to the concentration of the analyte, where C_{X_i} is the concentration of the analyte in the initial solution, $C_{S_f} + C_{X_f}$ is the concentration of the analyte plus the standard in the final solution, I_x is a sign of the initial solution and I_{S+X} is signal of the final solution. The deduction mechanism is given by Equation (5):

$$I_X = kC_{X_I} \tag{5}$$

$$I_{S+X} = k(C_{S_f} + C_{X_f}) \tag{6}$$

where k is a constant of proportionality. Dividing Eq. (5) by Eq. (6), we get Equation (7):

$$\frac{I_X}{I_{S+X}}=\frac{kC_{X_i}}{k\left(C_{S_f}+C_{X_f}\right)}=\frac{C_{X_i}}{\left(C_{S_f}+C_{X_f}\right)} \tag{7}$$

For an initial volume V_0 of the unknown sample and the added volume V_s of standard with concentration C_{S_i}, the total volume is $V = V_0 + V_s$ and the final concentrations in equation (6) are presented by Equations (8):

$$C_{X_f} = C_{X_i}\frac{V_0}{V} \tag{8a}$$

$$C_{S_f} = C_{S_i}\frac{V_S}{V} \tag{8b}$$

The dilution factor, V_0/V, is crucial in these calculations. By expressing the diluted concentration of the analyte C_{X_f} in terms of the initial concentration C_{X_i}, we can solve for C_{X_i}, given that all other variables are known.

Determining the concentration of ascorbic acid in pear-orange

Experimental data in Figure 10a shows that the anodic current is directly proportional to the concentration of AA. The addition of specific volumes of standard AA solution leads to corresponding increases in current.

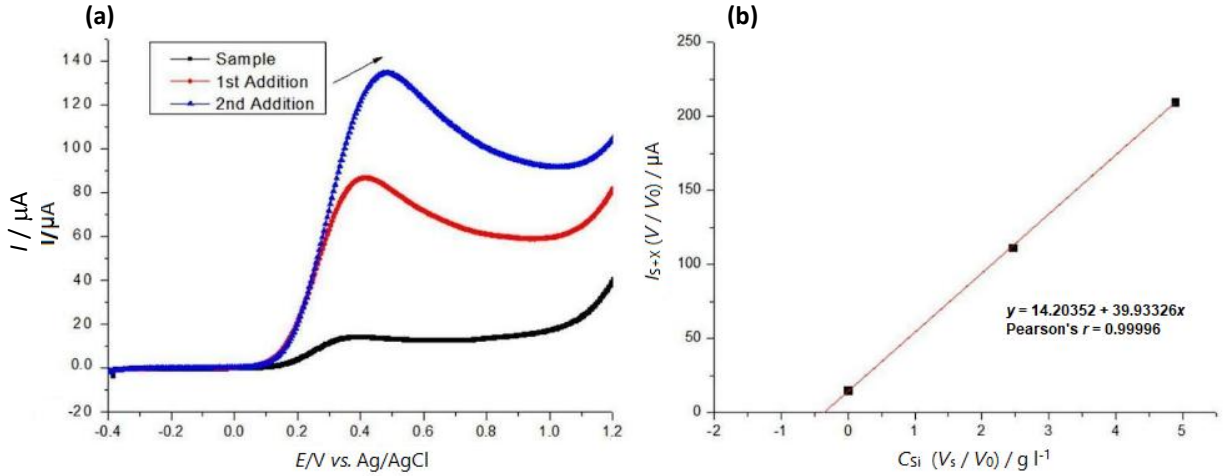

Figure 10. *(a) LSV curves at 50 mV s^{-1} of C-SPE in 0.1 mol L^{-1} phosphate buffer pH 5.5 and AA sample present in the juice of a pear-orange and two added volumes (5 and 10 µL) of 0.05 mol L^{-1} AA standard solution; (b) determination of AA concentration in pear-orange using standard addition method*

These data points and known parameters will be used to generate a linear equation for further analysis. A series of data points representing concentrations of standards added to the sample are calculated for the *x*-axis: C_{X_i} (V_S / V_0), and corresponding signals (I_{S+X}) adjusted for volume ratios, are calculated for the *y*-axis: I_{S+X} (V / V_0).

For the initial volume of unknown sample (V_0) = 0.018 mL and initial concentration of standard C_{S_i} = 0.05 M = 8.8 g L^{-1}, the needed parameters and calculated standard AA concentrations and corresponding currents are summarized in Table 1.

Table 1. *Analytical parameters and calculated concentrations of standards and resulting current responses for AA determination in pear-orange by standard addition method: V_0= 0.018 ml, C_{S_i} = 0.05 mol L^{-1} = 8.8 gL^{-1}*

V_S / mL	I_{S+X} / µA	V / mL	V_S / V_0	V / V_0	C_{S_i} (V_S / V_0) / g L^{-1}	I_{S+X} (V / V_0) / µA
0	14.72	0.018	0.000	1.00	0.00	14.72
0.0050	87.03	0.023	0.280	1.28	2.46	111.4
0.010	135.0	0.028	0.550	1.55	4.89	210.0

The linear Equation (9) shown in Figure 10b can be derived from the obtained data in Table 1:

$$y = 14.20352 + 39.93326x \quad (9)$$

Using Eq. (9), it can be easily calculated that for y = 0, x = |-0.36 g L^{-1}| = 0.36 g L^{-1} or 360 L^{-1}**.**

The experimental analysis revealed that the concentration of AA in the pear-orange sample was determined to be 360 mg L^{-1}. This value comes with a calculated uncertainty of ± 32.4 mg L^{-1}, which was derived using the propagated errors of the coefficients obtained from the software.

This result implies that the actual concentration of AA in pear oranges lies within the range of 327.6 to 392.4 mg L^{-1}.

Repeatability study

It's worth noting that variations in fruit variety may account for the observed differences in AA concentration. To validate the repeatability of this experiment, it was conducted in triplicate using two additional samples from the same batch of oranges.

To evaluate the repeatability of the analysis, the same orange juice sample underwent two additional LSV analyses. The entire initial procedure was repeated. The first repetition is referred to as duplicate analysis, and the second as triplicate analysis, yielding new peak potential and current values, which are presented below.

Duplicate analysis: Upon conducting the duplicate analysis (Figure 11a and 11b), the linear Equation (10) derived from the obtained data was:

$$y = 24.07257x + 6.80553 \quad (10)$$

Solving for x when y = 0, x = |-0.283 g L^{-1}| = 0.283 g L^{-1}.

The concentration of AA found in the pear-orange through duplicate analysis was determined to be 283 mg L^{-1}. This measurement comes with an associated uncertainty of ± 29 mg L^{-1}. Therefore, the experiment suggests that the concentration of AA within pear oranges is within the range of 254 to 312 mg L^{-1}.

Comparing this duplicate measurement to the value obtained in the initial analysis, the relative error ranged from -22.47 to -20.49 %. Notably, the concentration of AA in the duplicate analysis was lower than in the first assessment. However, it's essential to consider that both analyses were performed on the same orange, contributing to a reduced margin of error compared to literature data obtained from diverse experiments.

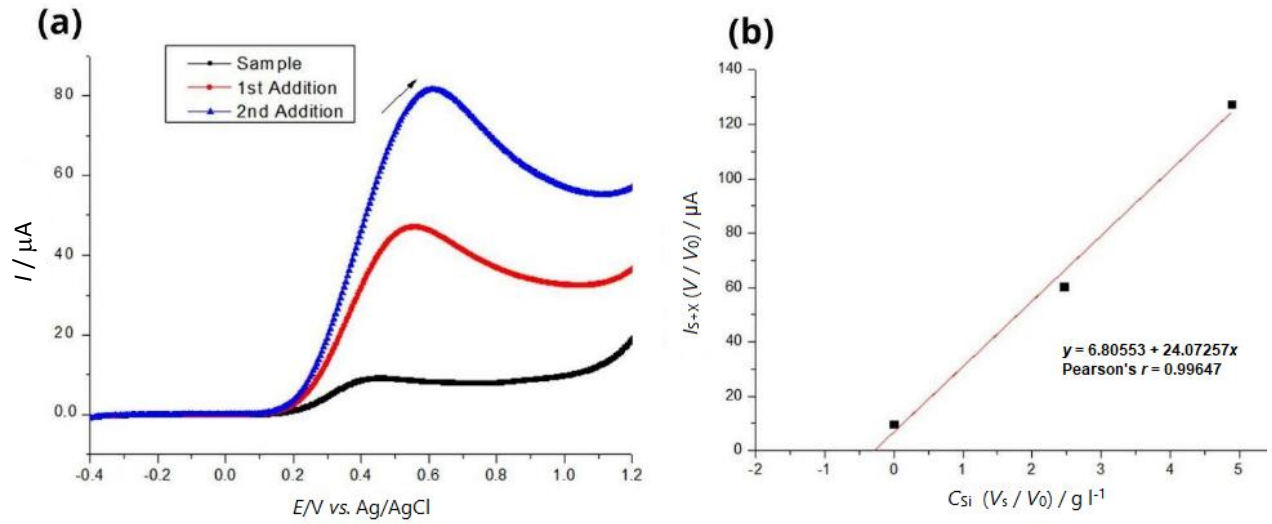

Figure 11. *LSV curves at 50 mV s^{-1} of C-SPE for a duplicate of the AA sample present in the juice of a pear-orange and for two added volumes of 0.05 mol L^{-1} AA standard solution, in 0.1 mol L^{-1}, phosphate buffer pH 5.5, scan rate 50 mV s^{-1}; (b) determination of AA concentration in duplicate pear-orange sample using standard addition method*

Triplicate analysis (Figures 12a and 12b): Using the linear fit equation, y = a + bx, it is possible to obtain Equation (11) from Fig. 12b:

$$y = 24.34109x + 6.521 \quad (11)$$

Solving for x when y = 0, we find that x = |-0.268 gL^{-1}| = 0.268 g L^{-1}.

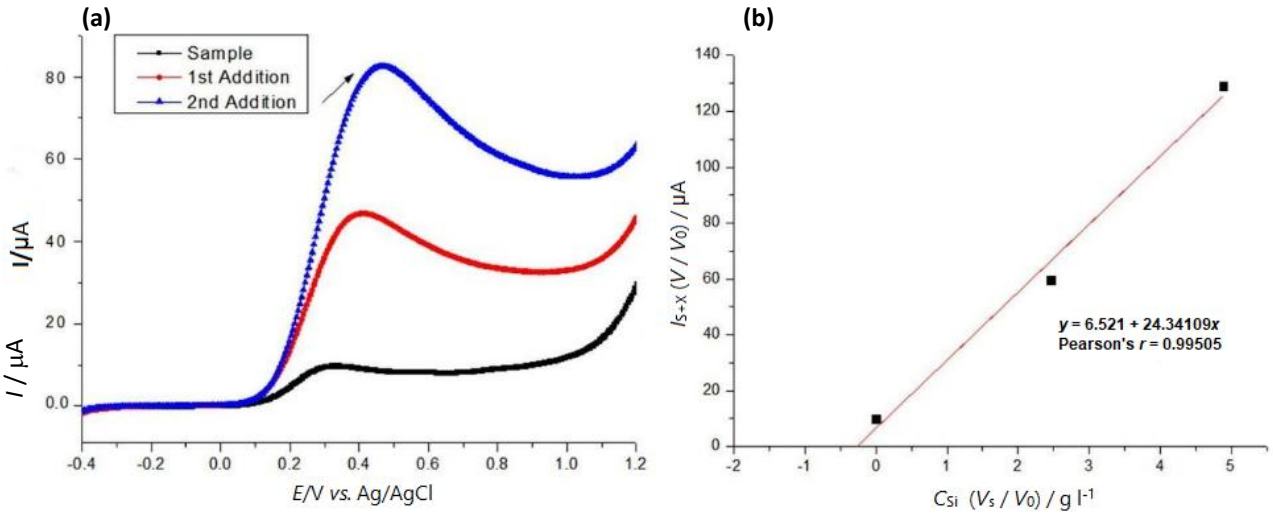

Figure 12. *LSV curves at 50 mV s^{-1} of C-SPE for a triplicate of the AA sample present in the juice of a pear-orange and for two added volumes of 0.05 mol L^{-1} AA standard solution in 0.1 mol L^{-1}, phosphate buffer pH 5.5; (b) determination of AA concentration in triplicate pear-orange sample using standard addition method*

The concentration of AA found in the pear-orange was quantified to be 268 mg L^{-1}, with an associated uncertainty of ± 34.2 mg L^{-1}. Based on this experiment, it can be inferred that the concentration of AA in pear-orange ranges from 233.8 to 302.2 mg L^{-1}. The standard deviation calculated for the three concentration values obtained was 49.36 mg L^{-1}.

Comparing this triplicate analysis to the value obtained in the first measurement, the relative error ranged from -28.63 to -22.99 %. This indicates that the concentration of AA in the triplicate analysis was also lower than in the first assessment.

To include the error bar of the replicates, a graph was generated (Figure 13) of the mean of the values corresponding to the y-axis by the values of the x-axis - the same for the three measurements since the dilution factor is maintained: 0 for the sample, 0.28 for the first addition and 0.56 for the second addition).

From the graph, it is possible to obtain the linear Equation (12):

$$y = 11.20558 + 28.40392x \quad (12)$$

Setting $y = 0$, the equation was solved for x, yielding |-0.394| g L-1, whose modulus corresponds to 0.394 g L-1, accompanied by an uncertainty of ± 37.4 mgL^{-1}. The relative error of this value compared to the literature is from -36.27 to -13.77 %.

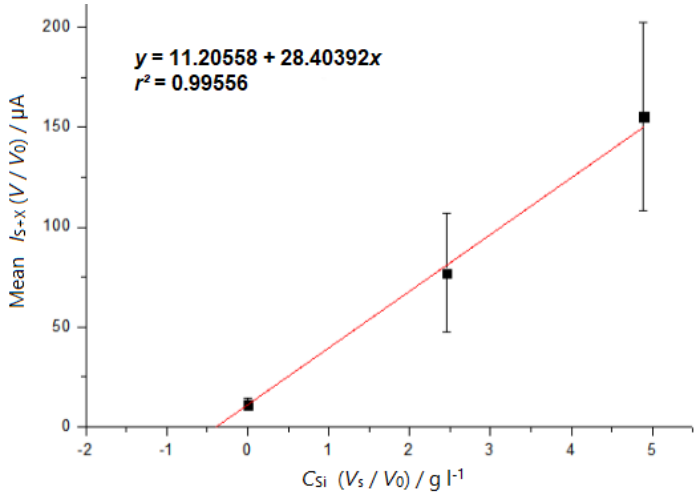

Figure 13. *Determination of AA concentration in pear-orange using the standard addition method with error bars considering the mean of three measurements*

Although the observed error, considering the three measurements, is reasonable (given the variety among the fruits themselves), when we look at each replicate individually, it is notable that in comparison to the duplicate analysis, the relative error of the triplicate was between -7.95 and -3.14 %. In other words, the concentration in the triplicate analysis was lower than in the first and second analyses. This discrepancy may be attributed to the degradation of AA over time, as these samples of juice originated from the same orange and were subjected to the environmental conditions of temperature, light, and oxygen. Hence, to ensure more precise results, the analyses conducted on Tahiti lemon and Ponkan tangerine were performed only once, preventing potential degradation of vitamin C due to prolonged exposure to ambient conditions.

Experimental determination of ascorbic acid concentration in Tahiti lemon

As seen in Figure 14a, the anodic currents measured at C-SPE in solutions containing juice sample of Tahiti lemon increase after additions of AA standard samples. For V_0 = 0.018 mL and C_{S_i} = 0.1 mol L^{-1} = 17.6 g L^{-1}, the needed parameters used for calculations of standard concentrations and corresponding currents are summarized in Table 2.

Table 2. *Analytical parameters and calculated concentrations of standards and resulting current responses for AA determination in Tahiti lemon by standard addition method:* V_0*= 0.018 ml,* C_{S_i} *= 0.1 mol* L^{-1} *= 17.6* gL^{-1}

V_S / mL	I_{S+X} / µA	V / mL	V_S / V_0	V / V_0	C_{S_i} (V_S / V_0) / g L^{-1}	I_{S+X} (V / V_0) / µA
0.000	17.67	0.018	0.000	1.00	0.00	17.67
0.005	51.00	0.023	0.280	1.28	4.89	65.17
0.010	74.21	0.028	0.550	1.55	9.78	115.4

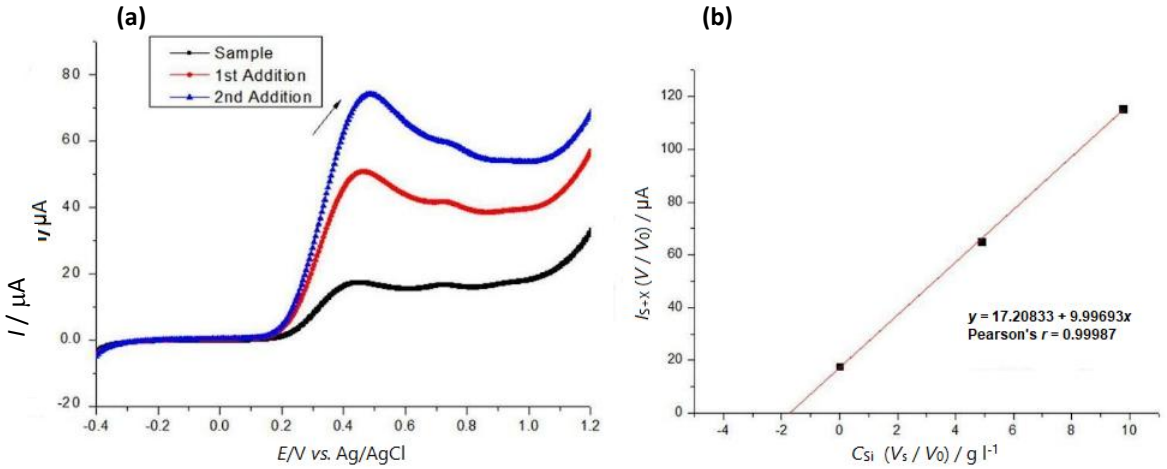

Figure 14. *(a) LSV curves at 50 mV s^{-1} of C-SPE in 0.1 mol L^{-1} phosphate buffer pH 5.5 containing AA sample present in Tahiti lemon juice and two added volumes (5 and 10 µL) of 0.01 mol L^{-1} AA standard solution; (b) determination of AA concentration in Tahiti lemon juice using standard addition method*

The linear equation derived from data in Table 2 and shown in Figure 14b is:

$$y = 17.20833 + 9.99693x \quad (13)$$

Setting $y = 0$, the equation was solved for x, yielding -1.72 g L^{-1}. This value was converted to a positive value, resulting in 1.72 g L^{-1}. Therefore, the concentration of AA in the Tahiti lemon was determined to be 1720 mg L^{-1}, accompanied by an uncertainty of ± 131.4 mg L^{-1}.

Thus, the experiment indicates that the concentration of AA present in the Tahiti lemon is between 1588.6 and 1851.4 mg L^{-1}. Compared to the TACO Table [12], the AA content in a lemon weighing approximately 100 g is around 38.2 mg. Therefore, considering that the lemon used yielded 35 mL and weighed 120 g (the theoretical value is 45.84 mg and the experimental value is within the range of 55.6 and 64.8 mg), the relative error presented had a range of 21.29 to 41.36 %.

Determining the concentration of ascorbic acid in Ponkan tangerine

LSV curves for C-SPE in a solution containing Ponkan tangerine juice are presented in Figure 15a. For V_0 = 0.018 mL and C_{S_i} = 0.05 mol L^{-1} = 8.8 g L^{-1} the needed analytical parameters for calculations of standard concentrations and corresponding currents are summarized in Table 3.

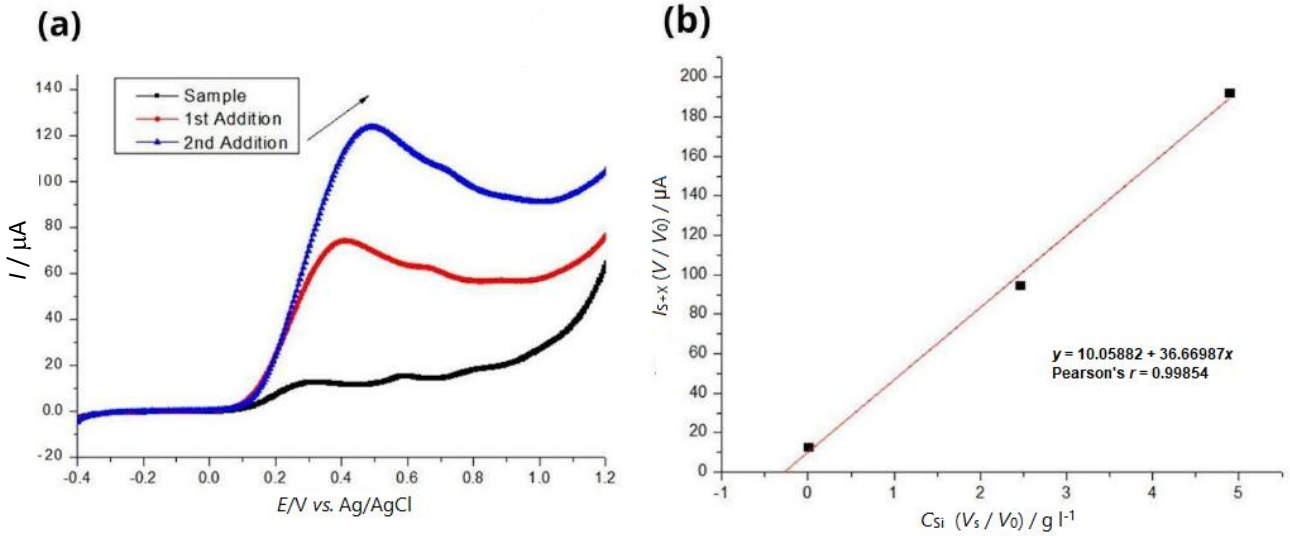

Figure 15. *(a) LSV curves at 50 mV s^{-1} of C-SPE in 0.1 mol L^{-1} phosphate buffer pH 5.5 containing AA sample present in Ponkan tangerine juice and two added volumes (5 and 10 µL) of 0.05 mol L^{-1} AA standard solution; (b) determination of AA concentration in Ponkan tangerine juice using standard addition method*

Table 3. *Analytical parameters and calculated standard concentrations and resulting current responses for AA determination in Ponkan tangerine by standard addition method:* V_0*= 0.018 ml,* C_{S_i} *= 0.05 mol* L^{-1} *= 8.8 g* L^{-1}

V_S / mL	I_{S+X} / µA	V / mL	V_S / V_0	V / V_0	C_{S_i} (V_S / V_0) / g L^{-1}	I_{S+X} (V / V_0) / µA
0.000	12.84	0.018	0.00	1.00	0.00	12.84
0.005	74.09	0.023	0.280	1.28	2.46	94.67
0.010	123.6	0.028	0.550	1.55	4.89	192.2

The linear Equation (14) derived from data in Table 2 and shown in Figure 15b is:

$$y = 10.05882 + 36.66987x \quad (14)$$

When $y = 0$, $x = -0.27$ g L^{-1}, equivalent to 0.27 g L^{-1}. Consequently, the concentration of AA found in the Ponkan tangerine was 270 mg L^{-1} with an uncertainty of ± 100 mg L^{-1}.

Thus, the experiment indicates that the concentration of AA present in the Ponkan tangerine is between 170 and 370 mg L^{-1}. Compared to the TACO table [13], the AA content in a Ponkan tangerine of approximately 100 g is around 48.8 mg. Therefore, considering that the tangerine used weighed 143.3 g (the theoretical value would be 69.93 mg) and yielded 60 mL of juice (experimental value between 10.2 and 22.2 mg), the relative error presented had a range of -85.4 to -68.2 %.

Again, the value found was lower (as with the pear-orange), which could be due to intra-species variation in the fruit itself but could also be due to losses during the procedure.

Conclusion

In summary, this study thoroughly evaluated the efficacy of various carbon electrodes (including the conventional glassy carbon electrode and highly sensitive carbon paste electrode) composed of graphite powder and paraffin, and the cost-effective commercial carbon screen-printed electrode. Among these, the C-SPE exhibited good performance in terms of anodic peak current, demonstrating its robustness, cost-effectiveness, and ease of use, thus positioning it as a compelling alternative for practical applications.

The effectiveness of the C-SPE was validated through its successful application in determining vitamin C concentrations in different citrus fruit samples using the standard addition method in conjunction with linear sweep voltammetry. The results for the ascorbic acid concentration in pear-orange ranged from 327.6 to 392.4 mg L^{-1} in the first analysis, as subsequent analyses were affected by degradation. For Tahiti lemon and Ponkan tangerine, the concentrations were 1588.6 to 1851. mg L^{-1} and 170 to 370 mg L^{-1}, respectively. These findings indicate that, among the fruits analyzed, Tahiti lemon is the richest source of vitamin C, making its consumption highly recommended for individuals needing to supplement this vitamin.

The applied voltammetric method, specifically LSV, for ascorbic acid determination, proved to be highly sensitive, rapid, and reproducible, particularly given the inherent variability among different fruit samples. These results underscore the considerable potential of C-SPE for practical applications in vitamin C analysis. Moreover, the development and utilization of specialized electrodes, such as C-SPE, reflect a broader trend in the field of food analysis, enhancing both precision and efficiency in nutrient quantification.

Acknowledgments: *The authors are thankful to CAPES (CAPES, PROCAD-SPCF - File number process 88887.613955/2021-00), FAPESP (File numbers 2017/22401-8 and 2022/12189-0), and CNPq (File number 302742/2022-0) for financial support. The authors also thank Dr. Cynthia Maria de Campos Prado Manso, who revised and edited this full text.*

References

[1] A. M. Pisoschi, A. Pop, A. I. Serban, C. Fafaneata, Electrochemical methods for ascorbic acid determination, *Electrochimica Acta* **121** (2014) 443-460. https://doi.org/10.1016/j.electacta.2013.12.127

[2] K. R. O. Araújo, Study on the determination of ascorbic acid in solution using a Nafion®-modified glassy carbon electrode, Master's Dissertation in Chemistry, Federal University of Goiás, Goiânia, Brazil, 2017.

[3] A. K. Alkhawaldeh, Platinum nanoparticle electrode modified iodine using cyclic voltammetry and chronoamperometry for determination of ascorbic acid, *Analytical and Bioanalytical Electrochemistry* **12(6)** (2020) 780-792. https://www.abechem.com/article_43202.html

[4] A. Pardakhty, S. Ahmadzadeh, S. Avazpour, V. Kumar Gupta, Highly sensitive and efficient voltammetric determination of ascorbic acid in food and pharmaceutical samples from aqueous solutions based on nanostructure carbon paste electrode as a sensor, *Journal of Molecular Liquids* **216** (2016) 387-391. https://doi.org/10.1016/j.molliq.2016.01.010

[5] J. G. Manjunatha, M. Deraman, G. P. Mamatha, Simultaneous voltammetric measurement of ascorbic acid and dopamine at poly (vanillin) modified carbon paste electrode: A cyclic voltammetric study, *Der Pharma Chemica* **4(6)** (2012) 2489-2497. https://www.derpharmachemica.com/pharma-chemica/simultaneous-voltammetric-measurement-of-ascorbic-acid-and-dopamine-at-poly-vanillin-modified-carbon-paste-electrode-a-c.pdf

[6] G. K. Jayaprakash, B. E. Kumara Swamy, S. C. Sharma, J. J. Santoyo-Flores, Analyzing electron transfer properties of ferrocene in gasoline by cyclic voltammetry and theoretical methods, *Microchemical Journal* **158** (2020) 105116. https://doi.org/10.1016/j.microc.2020.105116

[7] G. M. Alvez, A. S. Castro, B. R. McCord, M. F. de Oliviera, MDMA Electrochemical Determination and Behavior at Carbon Screen-printed Electrodes: Cheap Tools for Forensic Applications, *Electroanalysis* **33** (2021) 635-642. https://doi.org/10.1002/elan.202060080

[8] A. J. Bard, L. R. Faulkner, H. S. White, *Electrochemical methods: Fundamentals and Applications,* John Wiley & Sons, New York, USA, 2022. ISBN 978-1119334064. https://www.wiley.com/en-ae/Electrochemical+Methods%3A+Fundamentals+and+Applications%2C+3rd+Edition-p-9781119334057

[9] D. C. Harris, *Quantitative Chemical Analysis*, W. H. Freeman Publ., New York, USA, 2015. ISBN-978-1429218153

[10] D. A. Skoog, F. J. Holler, S.R. Courch, *Principles of Instrumental Analysis, 7th ed*., Cengage Learning, Boston, USA, 2017. ISBN: 978-1337468039

[11] N. A. S. Pereira, Characterization of carbon electrodes functionalized with perylene derivatives, Ph.D. Dissertation in Chemistry, University of Minho, Portugal, 2015. [Online]. Available: https://hdl.handle.net/1822/35644.

[12] G. F. S. Alegre, Determination of bioactive compounds and antioxidant capacity in fresh and pasteurized orange juices, Master's Dissertation in Food and Nutrition, UNESP, Araraquara, Brazil, 2015. [Online]. Available: http://hdl.handle.net/11449/121868.

[13] TACO, Brazilian Food Composition Table, NEPA/UNICAMP, Campinas, Brazil, 2011. [Online]. Available: https://www.cfn.org.br/wp-content/uploads/2017/03/taco_4_edicao_ampliada_e_revisada.pdf